Malaysian Journal of Analytical Sciences (MJAS)
Published by Malaysian Analytical Sciences Society

CRYSTAL STRUCTURE AND HIRSHFELD SURFACE ANALYSIS OF COMPOUND DI[2-((1E)-{2-(2-METHYLBENZYLSULFANYL) METHYLIDENE- HYDRAZIN-1-YLIDENE}METHYL)-6-METHOXY- PHENOL]

(Struktur Hablur dan Analisis Permukaan Hirshfeld bagi sebatian Di[2-((1E)-{2-(2-Metilbenzilsulfanil)Metiliden-Hidrazin-1-Iliden}Metil)-6-Metoksi-Fenol])

Enis Nadia Md Yusof[1*], Suhana Arshad[2], Kwong Huey Chong[3], and Siti Syaida Sirat[4,5]

[1]*Chemical Sciences Programme, School of Distance Education, Universiti Sains Malaysia, 11800 Minden, Penang, Malaysia*
[2]*X-ray Crystallography Unit, School of Physics, Universiti Sains Malaysia, Penang 11800, Malaysia*
[3]*Department of Chemistry, Faculty of Science, Universiti Putra Malaysia, 43400 UPM Serdang, Selangor Darul Ehsan, Malaysia*
[4]*School of Chemistry and Environment, Faculty of Applied Sciences, Universiti Teknologi MARA, Cawangan Negeri Sembilan, Kampus Kuala Pilah, 72000 Kuala Pilah, Negeri Sembilan, Malaysia*
[5]*Atta-ur-Rahman Institute for Natural Product Discovery (AuRIns), Universiti Teknologi MARA, Kampus Puncak Alam, 42300 Bandar Puncak Alam, Selangor, Malaysia*

[*]*Corresponding author: enisnadia@usm.my*

Received: 19 June 2023; Accepted: 23 July 2023; Published: 22 August 2023

Abstract

In this work we report crystal structure and Hirshfeld surface analysis of compound di[2-((1*E*)-{2-(2-methylbenzylsulfanyl)methylidene- hydrazin-1-ylidene}methyl)-6-methoxy- phenol] (**HL**), which has a dimeric dithiocarbazate backbone. **HL** has a non-planar structure due to strong intra-bonds that create two S(6) graph-set motifs, preventing free rotation by locking its atoms in a nearly planar arrangement. The crystal packing involves intermolecular C—H···S and C—H···π interactions that form a two-dimensional sheet parallel to the *ac*-plane which extends into a three-dimensional network arrangement via π···π interactions involving the centroid of the phenyl ring. Hirshfeld surface analysis describes that the major contribution to the overall crystal packing is from H···H contacts, followed by H···C/C···H contacts, which signify the presence of C—H···π interactions. The presence of intermolecular C—H···S interactions can be confirmed through the involvement of S···H/H···S contacts.

Keywords: dithiocarbazate, dimeric, crystal structure, Hirshfeld surface analysis

Abstrak

Dalam kajian ini, kami melaporkan struktur hablur dan analisis permukaan Hirshfeld bagi sebatian di[2-((1E)-{2-(2-metilbenzilsulfanil)metilidena-hidrazin-1-ilidena}metil)-6-metoksi-fenol] (**HL**), yang mempunyai rangkaian dithiocarbazat berbentuk dimerik. **HL** mempunyai struktur tidak rata disebabkan oleh ikatan dalaman yang kuat yang membentuk dua motif set-

graf S(6), menghalang putaran bebas dan mengunci atom-atomnya dalam susunan hampir rata. Penempatan hablur melibatkan interaksi intermolekul antara C—H···S dan C—H···π yang membentuk satu lapisan dua dimensi sejajar dengan satah *ac* dan meluas ke susunan rangkaian tiga dimensi melalui interaksi π···π yang melibatkan pusat gelang fenil. Analisis permukaan Hirshfeld menjelaskan bahawa sumbangan utama kepada penempatan kristal secara keseluruhan adalah daripada sentuhan H···H, diikuti oleh sentuhan H···C/C···H, yang menunjukkan kewujudan interaksi C—H···π. Kewujudan interaksi intermolekul antara C—H···S dapat disahkan melalui keterlibatan sentuhan S···H/H···S.

Kata kunci: dithiocarbazat, dimerik, struktur hablur, analisis permukaan Hirshfeld

Introduction

Dithiocarbazate Schiff bases have gained significant attention due to their diverse range of biological and pharmacological activities [1–5]. These compounds consist of a dithiocarbazate moiety (depicted in Figure 1), which is formed by condensing a primary amine with carbon disulfide and subsequently reacting it with an aldehyde or ketone to create the Schiff base. These ligands bear structural similarities to thiosemicarbazone and hydrazone ligands. Even minor modifications in the molecular structure of dithiocarbazate derivatives can result in intriguing biological properties [2, 6]. Moreover, these ligands possess both soft sulfur and hard nitrogen donor atoms, enabling them to coordinate with various metal ions to form metal complexes that exhibit fascinating physicochemical and enhanced biological characteristics. In this study, our focus lies on synthesizing di[2-((1E)-{2-(2-methylbenzylsulfanyl)methylidene- hydrazin-1-ylidene}methyl)-6-methoxy- phenol] (**HL**) and performing a single crystal X-ray diffraction (XRD) analysis to determine the crystal characteristics of **HL**. In addition, the significant intermolecular interactions have been studied using Hirshfeld surface analysis.

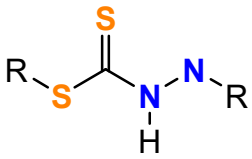

Figure 1. Dithiocarbazate backbone (R = alkyl/aryl/H)

Materials and Methods

Materials

Analytical reagent grade solvents and reagents were utilized without additional purification. The following chemicals were employed: Hydrazine hydrate (Fluka), 2-methylbenzyl chloride (ACROS), potassium hydroxide (HmbG), carbon disulfide (BDH), and 2-hydroxy-3-methoxybenzaldehyde (Merck). The solvents used were acetonitrile (Baker) and absolute ethanol with a purity of 99.8% (Scharlau).

Synthesis and crystallization of di[2-((1E)-{2-(2-methylbenzylsulfanyl)methylidene- hydrazin-1-ylidene} methyl)-6-methoxy- phenol] (HL)

The formation of the **HL** was synthesized using established literature procedures [4,7]. To initiate the synthesis, S-2-methylbenzyldithiocarbazate (2.12 g, 10 mmol) was dissolved in 100 mL of hot acetonitrile. This solution was then combined with an equimolar amount of 2-hydroxy-3-methoxybenzaldehyde (1.52 g, 10 mmol) dissolved in 20 mL of absolute ethanol. The resulting mixture was stirred at 80 °C for 30 minutes and allowed to sit at room temperature overnight. The completion of the reaction was checked using thin layer chromatography (TLC) plate. Following this, light yellow crystalline solid, 2-((1E)-{2-(2-methylbenzyl sulfanyl)methylidene-hydrazin-1-ylidene}methyl)-6-methoxy-phenol was obtained. The yellow crystalline solid was then recrystallized from a mixture of CH_3CN and EtOH in a 1:1 ratio. After several days of allowing the recrystallization solution to sit at room temperature, yellow plate-shaped crystals of the compound were formed. The single crystal X-ray diffraction analysis confirmed the unexpected product of di[2-((1E)-{2-(2-methylbenzylsulfanyl)methylidene- hydrazin-1-ylidene}methyl)-6-methoxy- phenol] (**HL**). The synthetic scheme for the formation of **HL** is shown in Scheme 1.

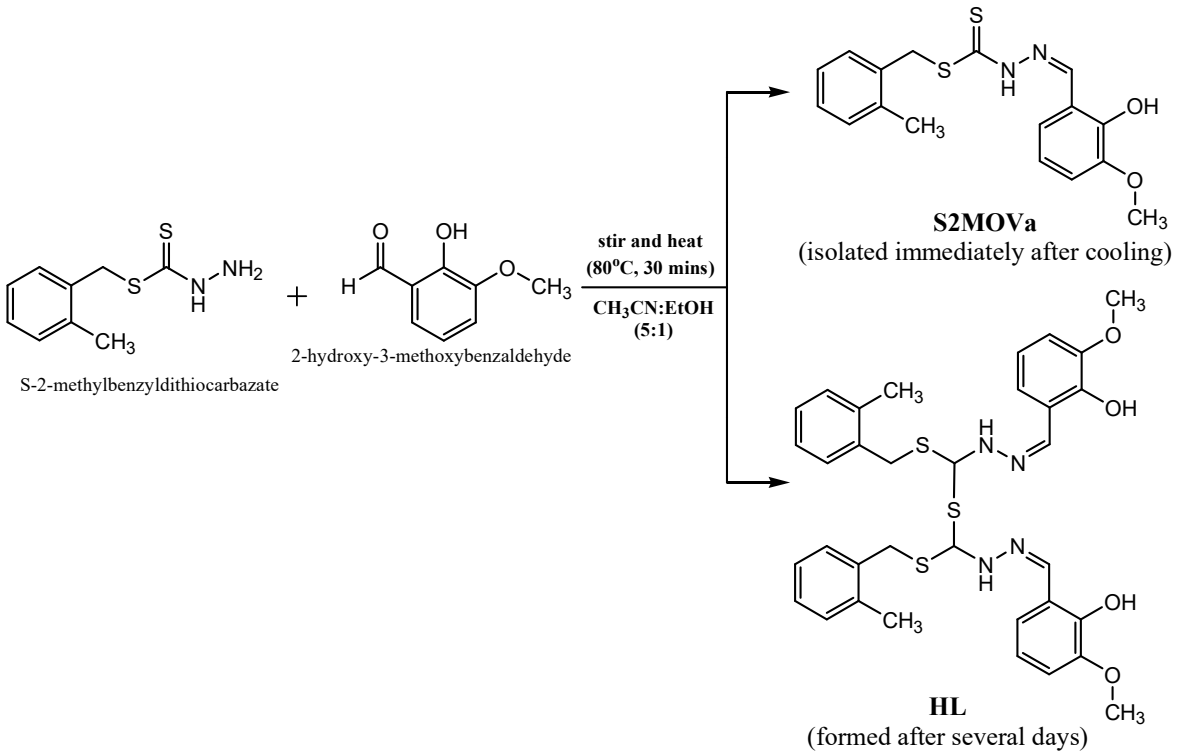

Scheme 1. Synthetic pathway for the formation of **HL**

X-ray crystallography refinement

X-ray analysis was conducted on a single crystal suitable for analysis using a CCD area-detector. CuKα radiation with a wavelength of 1.54178 Å was used. A high-quality crystal, clear and light yellow in color, measuring 0.58 × 0.31 × 0.15 mm, was carefully extracted and observed under a microscope for data collection. The APEX2 software was utilized for data collection, while cell refinement and data reduction were carried out using the SAINT software [8]. The crystal structure was solved using the Direct Method in the SHELXTL program and refined using its' full-matrix least squares technique on F^2 with anisotropic displacement parameters. Absorption correction was applied to the final crystal data using the SADABS software [8]. All geometric calculations were performed using the PLATON program [9]. Molecular graphics were generated using SHELXTL [10]. The non-hydrogen atoms were refined anisotropically, while the hydrogen atoms were positioned geometrically [C—H = 0.93, 0.96 or 0.97 Å] and refined using a riding model with isotropic displacement parameters set to 1.2 (for C) or 1.5 (for C_{methyl}) times the equivalent isotropic U values of the parent carbon atoms. The methyl groups were modelled using a rotating groups model. Additionally, hydrogen atoms bonded to oxygen atoms were located and distinguished through the differences observed through overlapping Fourier maps and freely refined [O-H = 0.76(4) and 0.81(4) Å]. In the final refinement, three outliers (991, 913, and 912) were omitted for clarity. Table 1 provides a summary of the crystal data and relevant refinement parameters for the **HL**.

Hirshfeld surface analysis

Hirshfeld surface and 2D-fingerprint plots calculations were carried out using CrystalExplorer 17.5 [11] on crystal structure imported from CIF file. The Hirshfeld Surfaces for **HL** were mapped with normalized contact distances (d_{norm}), shape index and curvedness functions.

Table 1. Crystallographic refinement parameters of **HL**

Parameters	
CCDC deposition numbers	2072116
Molecular formula	$C_{34}H_{34}N_4O_4S_4$
Molecular weight	690.89
Crystal system	Triclinic
Space group	*P*-1
a/Å	9.5955 (6)
b/Å	11.5562 (14)
c/Å	16.3622 (12)
α/°	71.797 (8),
β/°	88.527 (6),
γ/°	84.712 (7)
V/ Å^3	1716.2 (3)
Z	2
D_{calc} (Mg m^{-3})	1.337
μ (mm^{-1})	2.90
Radiation λ (Å)	1.54178
F(000)	724
Reflections measured	27271
Ranges/indices (*h*, *k*, *l*)	*h* = −11→11 *k* = −14→13 *l* = −20→20
θ limit (°)	4.0-71.7
Unique reflections	6608
Observed reflections ($I > 2\sigma(I)$)	5939
Parameters	427
R_1 [a], wR_2 [b] [$I \geq 2\sigma(I)$]	0.056/0.177
Goodness of fit [c] on F^2	1.10
R_{int}	0.049
Largest diff. peak and hole, e/Å^{-3}	0.66 and −0.35

w = $1/[\sigma^2(F_o^2) + (0.1009P)^2+1.0249P]$, where $P = (F_o^2 + 2F_c^2)/3$; [a] $R = \Sigma||F_o| - |F_c||/\Sigma|F_o|$, [b] $wR = \{w\Sigma(|F_o| - |F_c|)^2/\Sigma w|F_o|^2\}\}^{1/2}$, [c] $GOF = \{\Sigma w(|F_o| - |F_c|)^2/(n-p)\}^{1/2}$, where *n* is the number of reflections and *p* the total number of parameters refined

Results and Discussion

Molecular structure and crystal packing of HL

The molecular structure of the compound **HL** with assigned atom-numbering scheme are presented in Figure 2. The molecular structure of **HL** is crystallized in Triclinic crystal system with *P*-1 space group. All selected bond lengths and angles listed in Table 2 are found within the normal ranges. **HL** consist of dimeric dithiocarbazate backbone with two terminal toluene and 2-methoxyphenol moieties. Intramolecular O1—H1O1···N2 and O3—H1O3···N4 hydrogen bonds are observed with the non-bonding distances (O···N) and the angles (O—H···N) of the intramolecular hydrogen bond of 2.642(3 Å) Å, 159(5)° and 2.679(3) Å, 151(5)°, respectively. Subsequently, these bonds create two *S*(6) graph-set motif, preventing any free rotation of atom, hence locking them (O1/N2/C9-C11 and O3/N4/ C24-C26) in a nearly planar arrangement. Both sulphur and nitrogen bond lengths are found within the normal range where S1—S3 bond length is 2.0411 (9) Å and the N1—N2 as well as N3—N4 bond lengths are 1.406 (3) Å and 1.408 (3) Å, respectively. Figure 2 shows the non-planar

structure of **HL** where the terminal methyl substituted benzene rings are twisted at C1—S2—C2—C3 and C16—S4—C17—C18 torsion angles of −151.6 (2)° and −159.8 (2)°, respectively. Moreover, the terminal 2-methyl phenol rings are likewise observed to be twisted at C1—N1—N2—C9 torsion angle of −156.7 (2)° whereas on the other side of the molecule, the ring is observed to be slightly twisted with C16—N3—N4—C24 torsion angle of −173.9 (2)°. Additionally, the dihedral angles between the phenyl rings (Table 3) are also compared whereby the angles are in the range of 20°-72°, which further confirms the non-planar structure of **HL**.

In the arrangement of the crystal structure as shown in Figure 3 and Table 4, the molecules of **HL** are connected in a one-dimensional chain along the *a*-axis through intermolecular C7—H7···S3 hydrogen bonding. These intermolecular C—H···S interactions are further reinforced by intermolecular C—H···π interactions, specifically C19—H19···*Cg*2 (as indicated in Table 4), where *Cg*2 represents the centroid of the C25-C30 phenyl rings. These interactions result in the formation of a two-dimensional sheet parallel to the *ac*-plane. Furthermore, the crystal structure is strengthened by π···π interactions involving the centroid of the phenyl ring, *Cg*2 (C10-C15),where the centroid to centroid distance is 3.6423(16) Å. These π···π interactions results into extending the two-dimensional *ac*-sheets into a three-dimensional network arrangement.

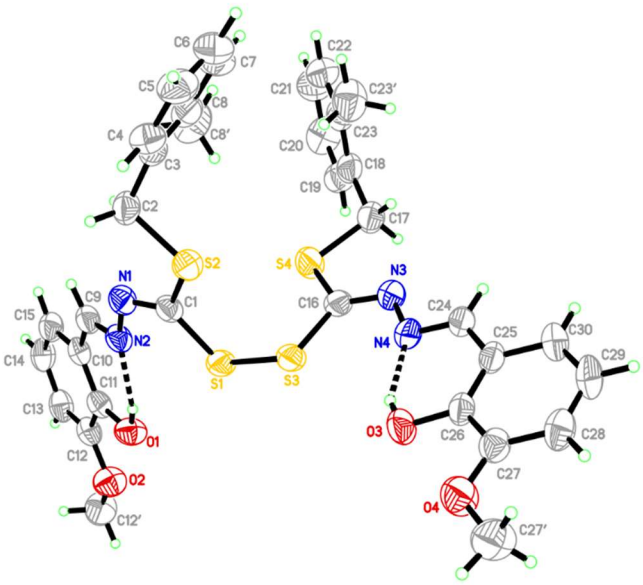

Figure 2. The molecular structure of **HL** with 50% ellipsoids probability with atomic numbering scheme. The dashed lines represent the intramolecular O—H···N hydrogen bonds.

Table 2. Selected bond lengths (Å), bond angle and torsion Angles (°) of **HL**

Bond Length (Å)		**Bond Angle (°)**		**Torsion Angle (°)**	
S1—C1	1.794 (3)	C1—S1—S3	104.56 (9)	C1—N1—N2—C9	−156.7 (2)
S1—S3	2.0411 (9)	C1—S2—C2	101.34 (13)	C16—N3—N4—C24	−173.9 (2)
S2—C1	1.744 (3)	C16—S3—S1	104.80 (9)	N2—N1—C1—S2	179.86 (18)
S2—C2	1.833 (3)	C16—S4—C17	100.72 (14)	N2—N1—C1—S1	2.6 (3)
S3—C16	1.789 (3)	C12—O2—C12′	117.0 (3)	C2—S2—C1—N1	−5.2 (3)
S4—C16	1.744 (3)	C27—O4—C27′	117.0 (3)	C2—S2—C1—S1	172.15 (16)
S4—C17	1.830 (3)	C1—N1—N2	112.1 (2)	S3—S1—C1—N1	177.5 (2)
O1—C11	1.360 (3)	C9—N2—N1	113.4 (2)	S3—S1—C1—S2	0.04 (17)
O2—C12′	1.431 (4)	C16—N3—N4	113.0 (2)	C1—S2—C2—C3	−151.6 (2)
O3—C26	1.352 (3)	C24—N4—N3	112.6 (2)	S2—C2—C3—C4	−89.6 (3)
O4—C27	1.361 (4)	N1—C1—S2	122.3 (2)	N1—N2—C9—C10	−179.3 (2)
O4—C27′	1.428 (4)	N1—C1—S1	120.4 (2)	N2—C9—C10—C11	4.3 (4)
N1—C1	1.273 (3)	S2—C1—S1	117.30 (14)	N4—N3—C16—S4	179.39 (19)
N1—N2	1.406 (3)	C3—C2—S2	105.05 (18)	N4—N3—C16—S3	1.4 (3)
N2—C9	1.285 (4)	C3—C8—C8′	122.1 (3)	C17—S4—C16—N3	0.7 (3)
N3—C16	1.280 (4)	N2—C9—C10	121.8 (3)	C17—S4—C16—S3	178.70 (18)
N3—N4	1.408 (3)	N3—C16—S4	121.7 (2)	S1—S3—C16—N3	−170.1 (2)
N4—C24	1.278 (4)	N3—C16—S3	119.8 (2)	S1—S3—C16—S4	11.91 (18)
C2—C3	1.498 (4)	S4—C16—S3	118.51 (15)	C16—S4—C17—C18	−159.8 (2)
C17—C18	1.502 (4)	C18—C17—S4	108.5 (2)	N3—N4—C24—C25	−179.0 (2)
C9—C10	1.455 (4)	C18—C23—C23′	122.0 (3)	N4—C24—C25—C30	177.0 (3)
C24—C25	1.449 (4)	N4—C24—C25	122.9 (3)	O3—C26—C27—O4	−1.5 (4)
C8—C8′	1.506 (5)	O3—C26—C27	118.0 (3)		
C23—C23′	1.492 (5)				

Table 3. The dihedral angles between the phenyl rings

Ring-Ring	**Dihedral Angle (°)**
A-B	64.47 (15)
A-C	51.44 (17)
A-D	49.63 (16)
B-C	20.75 (16)
B-D	65.86 (15)
C-D	71.47 (17)
A-B	64.47 (15)

Ring A, B, C & D are C3-C8, C10-C15, C18-C23 and C25-C30, respectively

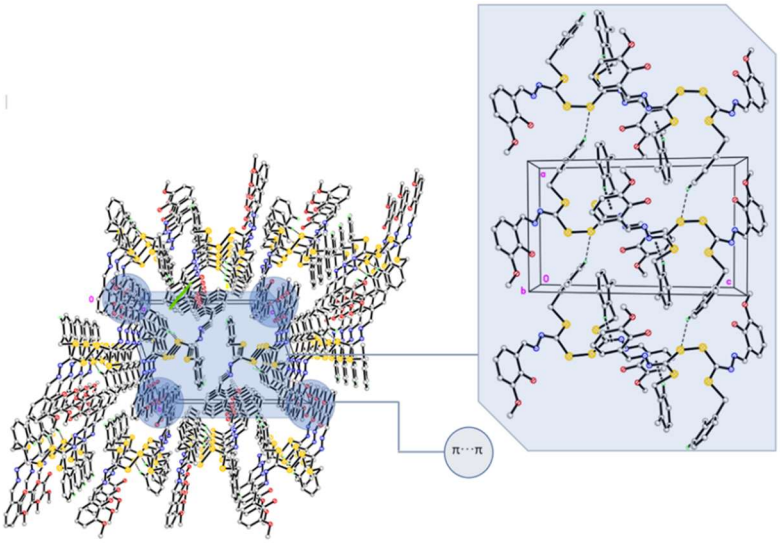

Figure 3. The crystal packing of **HL** showing a three-dimensional network molecular arrangement *via* intermolecular C—H···S, C—H···π and π···π interactions.

Table 4. Intra- and intermolecular hydrogen bonds and π···π interaction geometries (Å, °)

Bond	Bond Length, (Å)			Angle
D—H···A	D—H	H···A	D···A	D—H···A, (°)
O1—H1O1···N2	0.76(4)	1.92(4)	2.642(3)	159(5)
O3—H1O3···N4	0.81(4)	1.94(4)	2.679(3)	151(5)
C7—H7···S3^{i}	0.93	2.83	3.694(4)	155
C19—H19···*Cg*2^{ii}	0.93	2.78	3.607(4)	149
*Cg*1···*Cg*1^{iii}	-	-	3.6423(16)	-

(i) -1+*x*,*y*,*z*; (ii) 1-*x*,1-*y*,1-*z*; (iii) 1-*x*,-*y*,2-*z*. *Cg*1 and *Cg*2 is the centroid of C10-C15 and C25-C30, respectively

Hirshfeld surface analysis

Hirshfeld surface analysis was employed to conduct a thorough investigation of the intermolecular interactions within compound **HL**. This technique is highly valuable for visualizing and quantifying the diverse intermolecular interactions within the crystal structure. In Figure 4, the Hirshfeld surface is plotted using d_{norm}, enabling the visualization of intermolecular interactions through color codes (red, white, and blue). The red color signifies the closest or strongest contacts, indicating the sum of d_i (distance from a point on the surface to the nearest nucleus internal to the surface) and d_e (distance from a point on the surface to the nearest nucleus external to the surface), with de being shorter than the sum of the relevant Van der Waals radii. Conversely, weak intermolecular interactions are represented by white and blue color codes [12]. Notably, the dark red region surrounding each molecule corresponds to significant C—H···S interactions within the crystal packing. Additionally, the mapping of shape index and its curvature helps visualize π···π and C—H···π interactions involving phenyl rings. In Figure 5(a), the red concave regions exhibiting 'bow-tie' patterns on the shape index surface indicate the presence of aromatic stacking (π···π) interactions involving *Cg*1···*Cg*1, as well as the occurrence of C—H···π (C19—H19···*Cg*2) interactions. Figure 5(b) displays the Hirshfeld surface mapped over curvedness, highlighting flat surface patches characteristic of planar stacking involving *Cg*1···*Cg*1.

Furthermore, two-dimensional (2D) fingerprint plots are generated to provide quantitative information related to the type of intermolecular contacts present within the crystal [12,13]. The 2D fingerprint plots of Hirshfeld surfaces were successfully outlined into H···H, H···C/C···H, S···H/H···S, O···H/ H···O, H···N/N···H, C···C, N···C/C···N, O···C/C···O, S···N/N···S, N···N, S···C/C···S, and O···O contacts. The 2D fingerprint plots of the intermolecular contacts with their respective percentage contribution are presented in Figure 6. The H···H contacts contribute to the overall crystal packing at 42.6%. These dominant contacts may have attributed to the large hydrogen content of the molecule as observed through the exhibition of the two tips at $d_e + d_i$ = 2.3 Å. A pair of characteristic wings of H···C/C···H (22.3%) contacts at $d_e + d_i$ = 2.7 Å signifies the presence of C—H···π interactions in the compound. The existence of intermolecular C—H···S interactions can be confirmed through the involvement of 12.5% of S···H/H···S contacts as characterized by a pair of sharp peaks with spikes at $d_e + d_i$ = 2.7 Å. The H···N/N···H contacts contributing to about 3.7% in the Hirshfeld surface analysis is represented by a pair of diffuse spikes at $d_e + d_i$ = 2.8 Å. However, the weak C···C, N···C/C···N, O···C/C···O, S···N/N···S, N···N, S ···C/C···S, and O···O contacts minorly contributes in the **HL** compound with 2.7%, 1.7%, 0.9%, 0.6%, 0.4%, 0.3%, and 0.1%, respectively. All these intermolecular interactions aids in the stabilization of the **HL** molecular assembly [14].

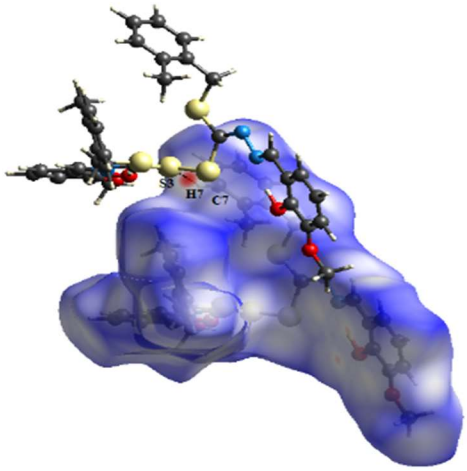

Figure 4. Hirshfeld surface mapped over d_{norm} showing hydrogen-bonding interaction with their neighbouring molecules

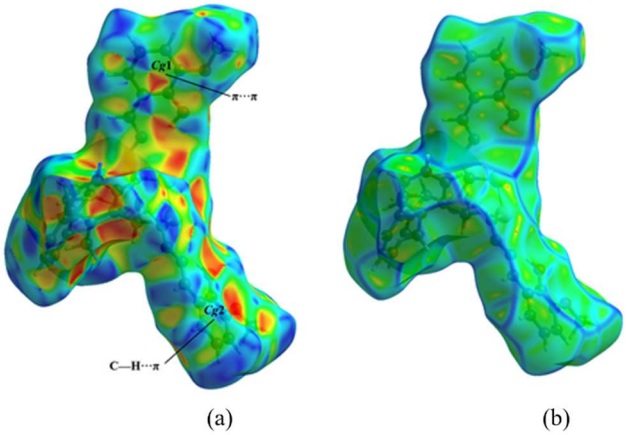

Figure 5. Hirshfeld surface mapped over (a) shape index and (b) curvedness

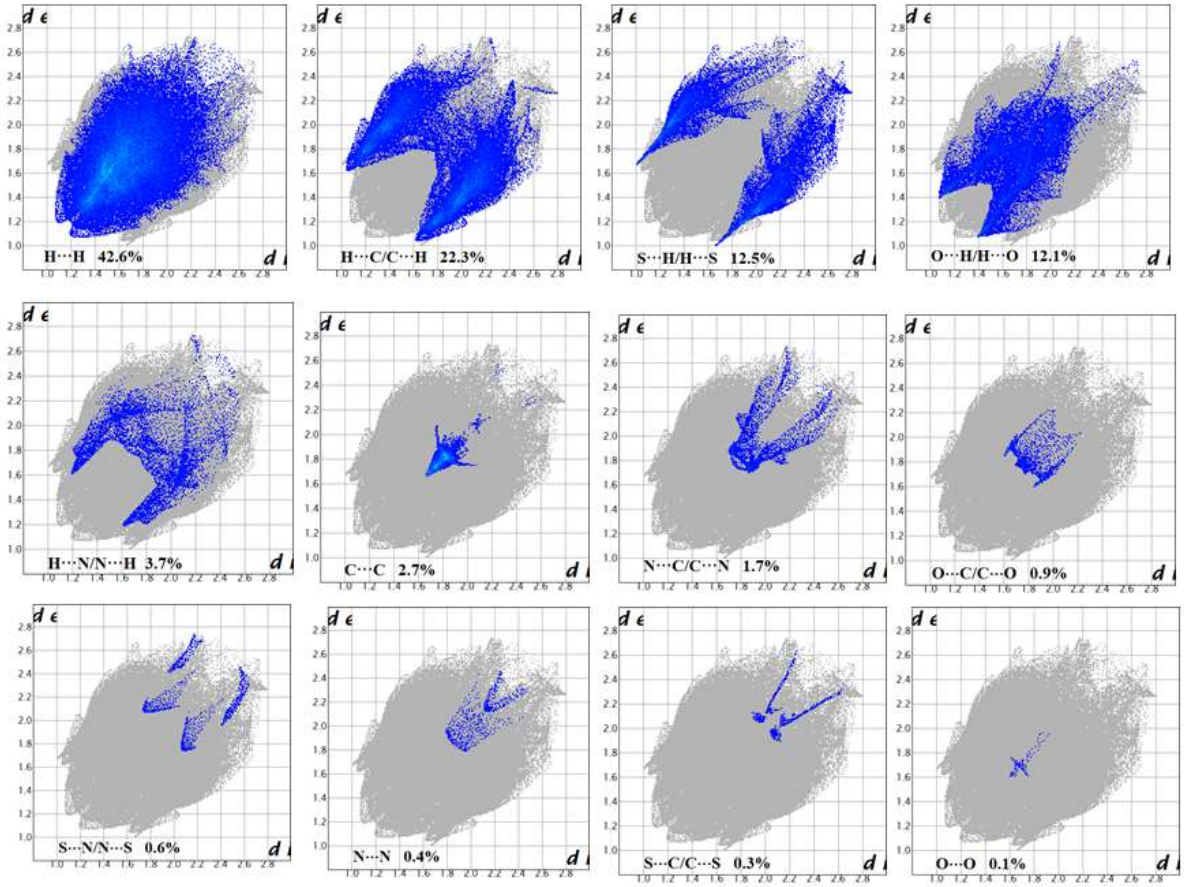

Figure 6. The 2D fingerprint plots of the intermolecular contacts with their respective percentage contribution

Database survey

There are three similar crystallographic literatures when compared to **HL** in the database, and the details are compiled in Table 5. Among them, Derivative (I) closely resembles **HL**, with the only difference being the S-bound R group. In Derivative (I), the S-bound R group is a S-methylbenzyl ester with a methyl group in the para position, and it has a 2-hydroxylbenzene ring bound to the imine-C. Figure 7 illustrates the close similarity between (I) and (II), where the only distinction lies in the S-bound R group, with R = *p*-methylbenzyl (GUPDAZ [15]) and R = H (LUGLUD [16]). Both (I) and (III) exhibit complete molecules generated by crystallographically imposed twofold symmetry, similar to **HL**. The S—S bond length of **HL** falls within the experimental range of 2.0373 (4) Å in (II) and 2.0504 (7) Å in (III). Similarly, the C—S—S—C torsion angle of **HL** exhibits the lowest angle compared to 90.70 (8) (I), (91.54 (6) (II), and 96.2 (1) (III). By comparing all the data, all four molecules mentioned in Table 5 adopt a similar conformation.

Table 5. Comparison of key geometric parameters (Å, °) in structures related to **HL**

Compound	Symmetry	S-S	C-S-S-C	Refcode	Reference
HL	2	2.0411 (9)	89.2(1)	-	This work
(I)	2	2.0439 (8)	90.70 (8)	GUPDAZ	[15]
(II)	-	2.0373 (4)	91.54 (6)	LUGLUD	[16]
(III)	2	2.0504 (7)	96.2 (1)	CUHHET	[17]

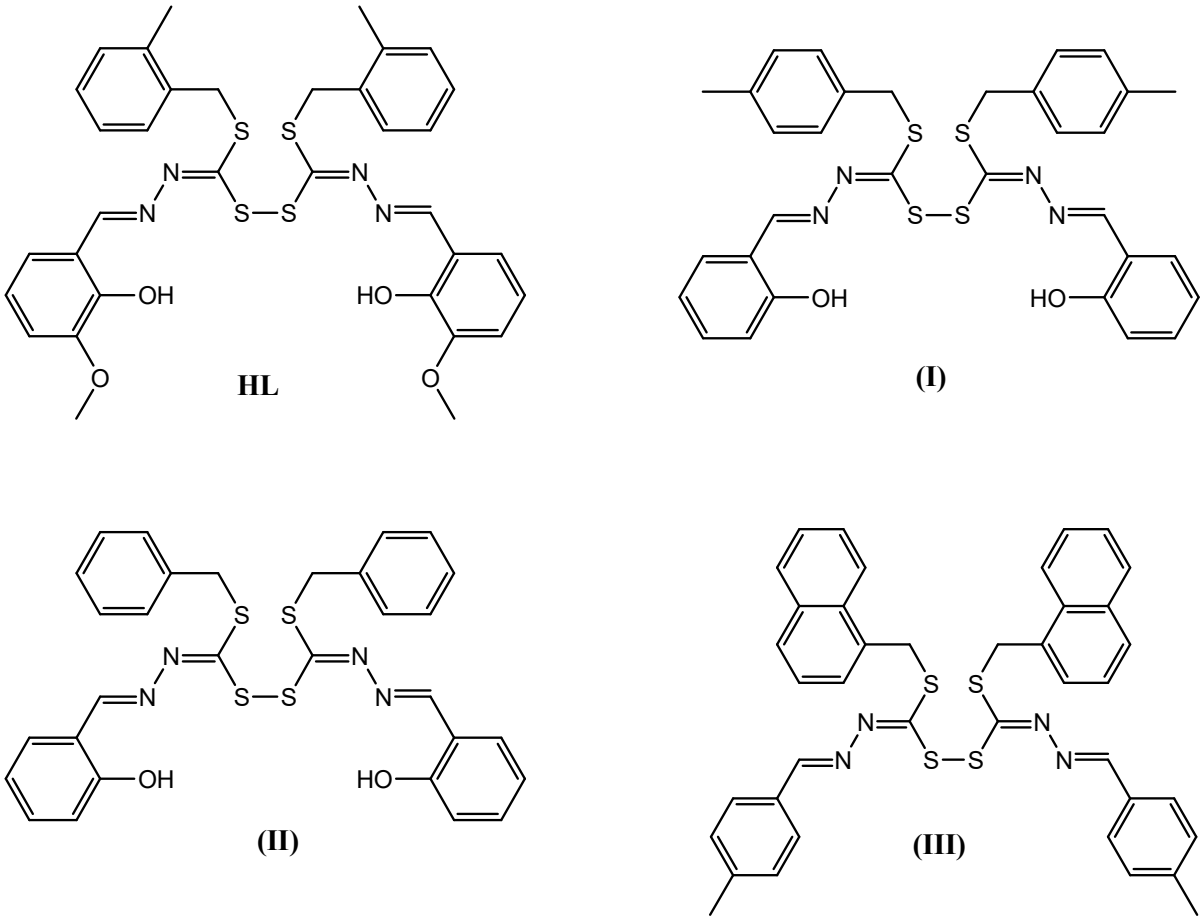

Figure 7. Molecular structures of **HL**, (I), (II), and (III)

Conclusions

A new structure of **HL** was synthesized and confirmed by single crystal X-ray diffraction analysis. The crystal system of the molecule was found to be triclinic, with the space group *P*-1. Furthermore, the Hirshfeld surface analysis revealed the existence of intriguing C—H···S intermolecular interactions within the crystal structure. Notably, the two-dimensional fingerprint plots emphasized the significance of H–H contacts, which accounted for the majority (42.6%) of the total Hirshfeld surface area. These findings shed light on the unique molecular arrangement and bonding patterns of **HL**, paving the way for further investigations into its properties and potential applications.

Appendix A. Supplementary data

CCDC No: 2072116 contains the supplementary crystallographic data of the synthesized compound. These data can be obtained free of cost via http://www.ccdc.cam.ac.uk/conts/retrieving.html, or from the Cambridge Crystallographic Data Centre, 12 Union Road, Cambridge CB2 1EZ, UK; fax: (+44) 1223–336–033; or e-mail: deposit@ccdc.cam.ac.uk.

Acknowledgements

The research described in this study was supported by the Short-Term Grant Scheme (304/PJJAUH/6315525) from Universiti Sains Malaysia. We express our gratitude to the School of Distance Education and School of Chemical Sciences at Universiti Sains Malaysia, as well as the Department of Chemistry at the Faculty of Science, Universiti Putra Malaysia (UPM), for providing the necessary facilities for this research. Additionally, we would like to acknowledge the valuable assistance of Dr. Thahira Begum, a former

associate professor at the Department of Chemistry, Faculty of Science, UPM, during this research project.

References

1. Li, M. X., Zhang, L. Z., Chen, C. L., Niu, J. Y., and Ji, B. S. (2012) Synthesis, crystal structures, and biological evaluation of Cu(II) and Zn(II) complexes of 2-benzoylpyridine Schiff bases derived from S-methyl- and S-phenyldithiocarbazates. *Journal of Inorganic Biochemistry,* 106: 117-125.
2. Bhat, R. A., Kumar, D., Alam, A., Mir, B. A., Srivastava, A., Malla, M. A., and Mir, M. A. (2018). Synthesis, characterization, thermal and DFT studies of S-methyl-β-N-(3-(2-nitrophenyl)allylidene)dithiocarbazate as anti-bacterial agent. *Journal of Molecular Structure*, 1173:72-80.
3. Santra, A., Brandao, P., Mondal, G., Bera, P., Jana, A., Bhattacharyya, I., Pramanik, C., and Bera, P. (2020). The role of methyl and benzyl substituted dithiocarbazate of 2-acetyl pyridine for the formation of bridged dimeric and unbridged monomeric copper(II) complexes and catecholase mimetic activity of the complexes. *Polyhedron*, 176:114277.
4. Yusof, E. N. M., Ravoof, T. B. S. A., Tiekink, E. R. T., Veerakumarasivam, A., Crouse, K. A., Tahir, M. I. M., and Ahmad, H. (2015). Synthesis, characterization and biological evaluation of transition metal complexes derived from N, S bidentate ligands, *International Journal of Molecular Sciences,* 16: 11034-11054.
5. Yusof, E. N. M., Latif, M. A. M., Tahir, M. I. M., Sakoff, J. A., Simone, M. I., Page, A. J., Veerakumarasivam A., Tiekink, E. R. T., and Ravoof, T. B. S. A. (2019). o-Vanillin derived Schiff bases and their organotin(IV) compounds: synthesis, structural characterisation, in-silico studies and cytotoxicity, *International Journal of Molecular Sciences,* 20: 854.
6. Zahan, R., Rahi, M. S., Sheikh, M. C., Miyatake, R., Zangrando, E., Naz, T., Islam, M. A. A. A. A., and Reza, M. A. (2019). Design, synthesis and X-ray structural studies of novel [acetonitrile-benzyl-3-N-(2, 4 dihydroxyphenylmethylene) hydrazine carbodithioato-κ3-N′, S, O] nickel(ll) complex that potently inhibit cell proliferation through regulation of apoptosis related genes, *Applied Organometallic Chemistry*, 33: 1-16.
7. Yusof, E. N. M., Ravoof, T. B. S. A., Jamsari, J., Tiekink, E. R. T., Veerakumarasivam, A., Crouse, K.A., Tahir, M. I. M., and Ahmad, H. (2015). Synthesis, characterization and biological studies of S-4-methylbenzyl-β-N-(2-furylmethylene)dithiocarbazate (S4MFuH) its Zn^{2+}, Cu^{2+}, Cd^{2+} and Ni^{2+} complexes, *Inorganica Chimica Acta.* 438: 85-93.
8. Blessing, R. H. (1995). An empirical correction for absorption anisotropy, *Acta Crystallographica Section A*, A51: 33-38.
9. Sheldrick, G. M. (2008) A short history of SHELX, *Acta Crystallographica Section A Foundations of Crystallography*, A64: 112-122.
10. Spek, A. L. (2009). Structure validation in chemical crystallography, *Acta Crystallographica Section D Biological Crystallography*, D65:148-155.
11. Spackman, P. R., Turner, M. J., McKinnon, J. J., Wolff, S. K., Grimwood, D. J., Jayatilaka, D. and Spackman, M. A. (2021). CrystalExplorer: A program for Hirshfeld surface analysis, visualization and quantitative analysis of molecular crystals. *Journal of Applied Crystallography*, 54(3): 1006-1011.
12. Spackman, M. A. and Jayatilaka, D. (2009). Hirshfeld surface analysis. *CrystEngComm*, 11(1): 19-32.
13. Melvin, M. K., Skelton, B. W., Eggers, P. K., and Raston, C. L. (2022). Synthesis, crystallization and Hirshfeld surface analysis of transition metal carboxylate pentapyridines, *CrystEngComm*, 24: 57-69.
14. Seth, S. K., Sarkar, D., Roy, A., and Kar, T. (2011). Insight into supramolecular self-assembly directed by weak interactions in acetophenone derivatives: Crystal structures and Hirshfeld surface analyses, *CrystEngComm*, 13: 6728-6741.
15. Paulus, G., Kwong, H. C, Crouse, K. A., and Tiekink, E. R. T. (2020). 2-[(1E)-[(Z)-2-({[(1Z)-[(E)-2-[(2-Hydroxyphenyl)methylidene]hydrazin-1-ylidene]({[(4-methylphenyl)methyl]sulfanyl})methyl] disulfanyl

}({[(4-methylphenyl)methyl]sulfanyl})methylidene)hydrazin-1-ylidene]methyl]phenol: Crystal structure, Hirshfeld surface anaanalysis and computational study. *Acta Crystallographica Section E: Crystallographic Communications*, 76:1245-1250.

16. Islam, M. A. A. A. A., Sheikh, M. C., Islam, M. H., Miyatake, R., and Zangrando, E. (2016). Crystal structure of 1,2-bis((benzylsulfanyl){2-[1-(2-hydroxyphenyl)ethylidene]hydrazin-1-ylidene}methyl) disulfane, *Acta Crystallographica Section E: Crystallographic Communications*, 72: 337-339.
17. How, F. N. F., Crouse, K. A., Tahir, M. I. M., and Watkin, D. J. (2009). Synthesis and structure determination of *S*,*S*'-(Naphthalen-2-ylmethyl sulfanyl (1-p-tolyl-ethylidene) hydrazine. *Journal of Chemical Crystallography*, 39: 894-897.